PCCP

PERSPECTIVE

View Article Online
View Journal | View Issue

Cite this: *Phys. Chem. Chem. Phys.*, 2018, **20**, 8411

Mechanisms ruling the partition of solutes in ionic-liquid-based aqueous biphasic systems – the multiple effects of ionic liquids†

Helena Passos, Teresa B. V. Dinis, Emanuel V. Capela, Maria V. Quental, Joana Gomes, Judite Resende, Pedro P. Madeira, Mara G. Freire and João A. P. Coutinho *

In the past decade, the remarkable potential of ionic-liquid-based aqueous biphasic systems (IL-based ABSs) to extract and purify a large range of valued-added biocompounds has been demonstrated. However, the translation of lab-scale experiments to an industrial scale has been precluded by a poor understanding of the molecular-level mechanisms ruling the separation or partition of target compounds between the coexisting phases. To overcome this limitation, we carried out a systematic evaluation of specific interactions, induced by ILs and several salts used as phase-forming components, and their impact on the partition of several solutes in IL-based ABSs. To this end, the physico-chemical characterization of ABSs composed of imidazolium-based ILs, three salts (Na_2SO_4, K_2CO_3 and $K_3C_6H_5O_7$) and water was performed. The ability of the coexisting phases to participate in different solute–solvent interactions (where "solvent" corresponds to each ABS phase) was estimated based on the Gibbs free energy of transfer of a methylene group between the phases in equilibrium, $\Delta G(CH_2)$, and on the Kamlet–Taft parameters – dipolarity/polarizability (π^*), hydrogen-bonding donor acidity (α) and hydrogen-bonding acceptor basicity (β) – of the coexisting phases. Relationships between the partition coefficients, the phase properties expressed as Kamlet–Taft parameters and COSMO-RS descriptors were established, highlighting the ability of ILs to establish specific interactions with given solutes. The assembled results clearly support the idea that the partition of solutes in IL-based ABSs is due to multiple effects resulting from both global solute–solvent and specific solute–IL interactions. Solute–IL specific interactions are often dominant in IL-based ABSs, explaining the higher partition coefficients, extraction efficiencies and selectivities observed with these systems when compared to more traditional ones majorly composed of polymers.

Received 17th January 2018,
Accepted 22nd February 2018

DOI: 10.1039/c8cp00383a

rsc.li/pccp

Introduction

Aqueous biphasic systems (ABSs) have been investigated in liquid–liquid extraction processes, demonstrating particularly suitability for the separation of biomolecules since they are formed by two immiscible aqueous phases. They can be formed by mixing two polymers, a polymer and a salt, or two salts in aqueous media, and above a given concentration, the phase separation takes place.[1–3] Besides the conventional polymer-based ABSs, in 2003, Rogers and co-workers[4] demonstrated that ABSs could be created by mixing ionic liquids (ILs) and inorganic salts. After this proof of principle, in the following years, it was shown that IL-based ABSs present additional advantages over the polymer-based systems, namely lower viscosity, faster phase separation, and higher extraction efficiencies and tailored selectivity for a wide range of biomolecules. After more than a decade of studies, IL-based ABSs are nowadays considered one of the most promising media for the extraction and separation of a broad range of biocompounds.[5]

While very promising at the lab-scale, ABSs have faced limited industrial interest, and examples for their commercial application are few.[1–3,6,7] The use of ABSs at an industrial scale has been plagued by a poor understanding of the molecular-level mechanisms that rule the partition of the target solutes/biomolecules/products between the coexisting phases, limiting the ability to design ABSs for a specific application, and converting the development of novel ABS-based separation processes in a lengthy trial and error approach. With the purpose of improving

CICECO – Aveiro Institute of Materials, Department of Chemistry, University of Aveiro, 3810-193 Aveiro, Portugal. E-mail: jcoutinho@ua.pt

† Electronic supplementary information (ESI) available: Materials and experimental procedure, and detailed experimental data of binodal curves, DNP-amino-acid partition, Gibbs free energy and Kamlet–Taft parameters determination, and correlations between the several parameters. See DOI: 10.1039/c8cp00383a

the understanding of the partition of target products in ABSs, several works reporting insights on the physicochemical characterization of ABSs composed of polymer/polymer and polymer/salt combinations have been reported.[8–16] The consensus seems to be that the distribution of compounds in these more traditional ABSs is ruled by differences in solute–solvent interactions.[8]

Among the approaches available for the physicochemical characterization of ABSs, the Gibbs free energy of transfer of a methylene group between the phases and the Kamlet–Taft Linear Solvation Energy Relationship (LSER) have been successfully used for the description of the partition of solutes in ABSs composed of polymers and salts.[3,4,8–15,17–19] The relative affinity of the coexisting phases for methylene groups in ABSs has been shown to be an important factor controlling the molecule partition.[3,4,17–19] This property can be assessed through the analysis of the partition coefficients of a homologous series of compounds with aliphatic moieties of increasing length. The logarithm of partition coefficients is linearly dependent on the equivalent number of methylene groups in the alkyl side-chain, $n(CH_2)$, as described by eqn (1).

$$\ln(K) = C + E{\cdot}n(CH_2) \quad (1)$$

where the parameters C and E are characteristic constants for a given ABS. C corresponds to the partition of the non-alkyl moiety of the molecule, and it has been suggested to represent the difference in the polar/electrostatic properties of the phases, if sodium salts of dinitrophenyl-amino-acids (DNP-amino-acids) are partitioned. E is related to the Gibbs free energy of transfer of a methylene group between the phases in equilibrium, $\Delta G(CH_2)$, and it has been proposed as a measure of the relative hydrophobicity of the phases, given by the equation:[3]

$$\Delta G(CH_2) = -RTE \quad (2)$$

where R is the universal gas constant and T is the absolute temperature. $\Delta G(CH_2)$ has also been used as a measure of the free energy for cavity formation.[13]

Polarity is widely used to classify solvents and their solvation ability, and it is defined as the sum of all specific and non-specific interactions occurring between a solvent and a solute, without considering the interactions associated with solute chemical transformations.[20,21] Since it is impossible to describe the multiple solute–solvent interactions using a single parameter, Kamlet and Taft proposed a multiparametric approach based on a set of solvatochromic probes, allowing the assessment of different interactions for the same solvent,[22–24] such as its dipolarity/polarizability (π^*), and hydrogen bond donor (α) and hydrogen bond acceptor (β) abilities. These parameters allowed the development of correlations for the description of a variety of properties using the LSER model,[22–24] given by:

$$(XYZ) = (XYZ)_0 + s\pi^* + a\alpha + b\beta \quad (3)$$

where (XYZ) is the value for a particular solvent-dependent property, $(XYZ)_0$ is the value for the reference system, and s, a, and b are the solute-dependent coefficients characterizing the respective influence of π^*, α and β terms on the (XYZ) property under study.[22–24] There are several examples of the successful application of this approach to correlate properties of solvents and solvent mixtures.[8–14,25]

In addition to previous efforts concerning the physicochemical characterization of polymer/polymer and polymer/salt ABSs by the determination of the solvatochromic parameters and relative hydrophobicity of the coexisting phases,[8–10,14,15] their application in IL-based ABSs has been limited and hampered by experimental difficulties, as discussed below.[19,26–28] Although nowadays a large database is available for π^*, α, and β for pure ILs,[21,29–32] no solvatochromic parameters for the IL-based ABS phases are available and only relative hydrophobicities for a small number of systems have been reported.[19,26–28]

Due to the increased interest in IL-based ABSs for the extraction, separation and purification of value-added biomolecules and products,[5] the understanding of the mechanisms that rule the ABS formation and the solute partition in these systems is of extreme relevance in the design of effective separation systems that could ultimately be applied at an industrial scale. To overcome this limitation, we performed a comprehensive study on the physicochemical properties of ABSs composed of imidazolium-based ILs, three salts – K_2CO_3, Na_2SO_4, and $K_3C_6H_5O_7$ – and water. Different probes were used to assess the Kamlet–Taft parameters of the coexisting phases, namely their dipolarity/polarizability (π^*), hydrogen-bond acidity (α), and hydrogen-bond basicity (β). Additionally, the partition coefficients of a series of DNP-amino-acids were determined to infer the relative hydrophobicity and electrostatic properties of the coexisting phases. Finally, the relationship between the DNP-amino-acid partition coefficients and the phase properties as characterized by Kamlet–Taft parameters was assessed. COSMO-RS (COnductor-like Screening MOdel for Real Solvents) parameters were used to complement these correlations and to evaluate the relevance of solute–IL specific interactions.

Experimental

Materials

ABS composed of several ILs and salts, namely K_2CO_3 (99 wt% pure from Sigma-Aldrich), Na_2SO_4 (99.82 wt% pure from José Manuel Gomes dos Santos, LDA), and $K_3C_6H_5O_7$ monohydrated ($\geq$99 wt% pure from Sigma-Aldrich), were studied. The following ILs were used: 1-butyl-3-methylimidazolium trifluoromethanesulfonate, $[C_4C_1im][CF_3SO_3]$ (99 wt%), 1-butyl-3-methylimidazolium thiocyanate, $[C_4C_1im][SCN]$ (>98 wt%), 1-butyl-3-methylimidazolium tosylate, $[C_4C_1im][TOS]$ (99 wt%), 1-butyl-3-methylimidazolium dicyanamide, $[C_4C_1im][N(CN)_2]$ (>98 wt%), 1-butyl-3-methylimidazolium ethylsulfate, $[C_4C_1im][C_2H_5SO_4]$ (98 wt%), 1-butyl-3-methylimidazolium methylsulfate, $[C_4C_1im]$-$[CH_3SO_4]$ (99 wt%), 1-butyl-3-methylimidazolium bromide, $[C_4C_1im]Br$ (99 wt%), 1-butyl-3-methylimidazolium dimethylphosphate, $[C_4C_1im][DMP]$ (>98 wt%), 1-butyl-3-methylimidazolium methylacetate, $[C_4C_1im][CH_3CO_2]$ (>98 wt%), 1-butyl-3-methylimidazolium methanesulfonate, $[C_4C_1im][CH_3SO_3]$ (98 wt%), 1-butyl-3-methylimidazolium chloride, $[C_4C_1im]Cl$

(99 wt%), and 1-butyl-3-methylimidazolium octylsulfate, $[C_4C_1im][C_8H_{17}SO_4]$ (>95 wt%). The chemical structures of the cation and the different anions that comprise the studied ILs are given in the ESI.† With the exception of $[C_4C_1im][C_8H_{17}SO_4]$ that was acquired from Aldrich, all remaining ILs were purchased from Iolitec. To reduce the water and volatile compound content to negligible values, IL individual samples were dried under constant stirring at vacuum and moderate temperature (≈323 K) for a minimum of 48 h. After this step, the purity of each IL was checked by ^1H and ^{13}C NMR and found to be in accordance with the purity given by the suppliers. Phosphate buffered saline (PBS) tablets from Sigma were used to buffer the aqueous solutions used in Na_2SO_4-based ABSs to a pH of 7.4. Four dinitrophenylated (DNP)-amino-acids were used in the Gibbs free energy determination: *N*-(2,4-dinitrophenyl)glycine (≥98 wt% pure) and *N*-(2,4-dinitrophenyl)-L-valine (>98 wt% pure), obtained from Sigma-Aldrich, and *N*-(2,4-dinitrophenyl)-L-alanine (>98 wt% pure) and *N*-(2,4-dinitrophenyl)-L-leucine (>99 wt% pure), supplied by Tokyo Chemical Industry (TLC). The probes *N*,*N*-diethyl-4-nitroaniline, 99% purity from Fluorochem, 4-nitroaniline, 99% purity from Aldrich, and pyridine-*N*-oxide, 95% purity from Aldrich, were used as received. Double distilled water was used.

Phase diagrams and tie-lines

The limit between the monophasic and biphasic regions, *i.e.* the solubility or binodal curves, for the studied systems was determined through the cloud point titration method[33] at (25 ± 1) °C and atmospheric pressure. The systems composed of $K_3C_6H_5O_7$, water and $[C_4C_1im][CF_3SO_3]$, $[C_4C_1im][SCN]$, $[C_4C_1im][N(CN)_2]$, $[C_4C_1im]Br$ and $[C_4C_1im]Cl$ were previously reported by Passos *et al.*[34] For the remaining systems, aqueous solutions of K_2CO_3 at 50 wt%, Na_2SO_4 at 20 wt%, and $K_3C_6H_5O_7$ at 50 wt%, and aqueous solutions of the different $[C_4C_1im]$-based ILs at variable concentrations were prepared gravimetrically and used for the determination of the respective binodal curves. In the preparation of the solutions for the determination of the Na_2SO_4-based ABSs, a PBS solution (0.01 M phosphate buffer, 0.0027 M potassium chloride and 0.137 M sodium chloride) was used instead of pure water, mainly to keep the pH at values close to 7. Repetitive drop-wise addition of the salt solution to each IL aqueous solution was carried out until the detection of a cloudy mixture. Then, repetitive drop-wise addition of double distilled water was carried out until the detection of a clear and limpid mixture. Drop-wise additions were performed under constant stirring. The ternary system compositions corresponding to the description of the phase diagrams were determined by weight quantification of all components added to the mixture, within $\pm 10^{-4}$ g.

Tie-lines (TLs) were determined by a gravimetric method originally described by Merchuk *et al.*[35] A mixture composition at the biphasic region was gravimetrically prepared, vigorously stirred, and allowed to reach the equilibrium by the separation of the phases for at least 12 h at (25 ± 1) °C. Both top and bottom phases were then weighed. Finally, each individual TL was determined by the application of the lever-arm rule.

The experimental binodal curves were fitted according to eqn (4):

$$[\mathrm{IL}] = A\exp[(B \times [\mathrm{salt}]^{0.5}) - (C \times [\mathrm{salt}]^3)] \quad (4)$$

where [IL] and [salt] correspond to IL and salt weight fraction percentages, respectively; and A, B and C are constants obtained by the least-squares regression of the experimental data.

For the determination of TLs, the following system of four equations (eqn (5)–(8)) was used with four unknown variables ($[IL]_{IL}$, $[salt]_{IL}$, $[IL]_{salt}$, and $[salt]_{salt}$), according to a set of premises (eqn (9)–(11)):

$$[\mathrm{IL}]_{\mathrm{IL}} = A\exp[(B \times [\mathrm{salt}]_{\mathrm{IL}}^{0.5}) - (C \times [\mathrm{salt}]_{\mathrm{IL}}^3)] \quad (5)$$

$$[\mathrm{IL}]_{\mathrm{salt}} = A\exp[(B \times [\mathrm{salt}]_{\mathrm{salt}}^{0.5}) - (C \times [\mathrm{salt}]_{\mathrm{salt}}^3)] \quad (6)$$

$$[\mathrm{IL}]_{\mathrm{IL}} = \frac{[\mathrm{IL}]_{\mathrm{M}}}{\alpha} - \frac{1-\alpha}{\alpha} \times [\mathrm{IL}]_{\mathrm{salt}} \quad (7)$$

$$[\mathrm{salt}]_{\mathrm{IL}} = \frac{[\mathrm{salt}]_{\mathrm{M}}}{\alpha} - \frac{1-\alpha}{\alpha} \times [\mathrm{salt}]_{\mathrm{salt}} \quad (8)$$

$$w(\mathrm{IL})_{\mathrm{M}} = \frac{w_{\mathrm{IL}} \times [\mathrm{IL}]_{\mathrm{IL}}}{100} + \frac{w_{\mathrm{salt}} \times [\mathrm{IL}]_{\mathrm{salt}}}{100} \quad (9)$$

$$w(\mathrm{salt})_{\mathrm{M}} = \frac{w_{\mathrm{IL}} \times [\mathrm{salt}]_{\mathrm{IL}}}{100} + \frac{w_{\mathrm{salt}} \times [\mathrm{salt}]_{\mathrm{salt}}}{100} \quad (10)$$

$$\frac{[\mathrm{salt}]_{\mathrm{salt}} - [\mathrm{salt}]_{\mathrm{M}}}{[\mathrm{salt}]_{\mathrm{M}} - [\mathrm{salt}]_{\mathrm{IL}}} = \frac{w_{\mathrm{IL}}}{w_{\mathrm{salt}}} \quad (11)$$

where the indexes M, IL and salt correspond to the mixture, IL- and salt-rich phases, respectively. The parameter α is the ratio between the IL-rich phase and the total mixture weight. $w(IL)_M$ and $w(salt)_M$ are the amounts of IL and salt weighed for the mixture point preparation, while w_{IL} and w_{salt} represent the weight of IL- and salt-rich phases, respectively. The solution of the referred system gives the concentration of IL and salt in the top and bottom phases.

The tie-line length (TLL) was calculated according to eqn (12).

$$\mathrm{TLL} = \sqrt{([\mathrm{salt}]_{\mathrm{IL}} - [\mathrm{salt}]_{\mathrm{salt}})^2 + ([\mathrm{IL}]_{\mathrm{IL}} - [\mathrm{IL}]_{\mathrm{salt}})^2} \quad (12)$$

DNP-amino-acid partition coefficients

Ternary mixture compositions were chosen based on the phase diagrams determined for each IL–K_2CO_3, IL–Na_2SO_4 and IL–$K_3C_6H_5O_7$ system. Moreover, to avoid discrepancies in the results that could arise from the different compositions of the phases, all the partitioning studies were performed at a constant TLL (≈50 for IL–K_2CO_3 and IL–$K_3C_6H_5O_7$, and ≈40 for IL–Na_2SO_4). Mixture compositions are given in Table 1. DNP-amino-acids were prepared in a concentration of 0.2 wt% in a PBS aqueous solution. For each mixture point, a total of six replicates were prepared in Eppendorf tubes containing different amounts of DNP-amino-acid stock solutions (0, 20, 40, 60, 80 and 100 μL). The Eppendorf tubes were stirred using an Eppendorf Thermomixer Comfort equipment at 1200 rpm

Table 1 Experimental data for TLs and TLLs of $[C_4C_1im]$-based ILs + salt + H_2O ABSs at 25 °C[a]

IL	Weight fraction composition/wt%						
	$[IL]_{IL}$	$[salt]_{IL}$	$[IL]_M$	$[salt]_M$	$[IL]_{salt}$	$[salt]_{salt}$	TLL
IL + K_2CO_3 + H_2O ABS							
$[C_4C_1im][CF_3SO_3]$	58.32	1.04	37.05	4.40	8.85	9.13	50.13
$[C_4C_1im][SCN]$	54.83	1.86	27.78	8.77	3.96	14.97	52.91
$[C_4C_1im][TOS]$	45.96	4.19	26.85	10.27	6.29	16.81	41.62
	46.91	3.99	28.34	10.16	4.28	18.16	44.92
	50.46	3.31	26.85	12.01	1.37	21.40	52.32
	53.31	2.82	28.01	12.21	0.96	22.25	55.85
	55.81	2.43	29.55	12.25	0.67	23.05	58.86
$[C_4C_1im][N(CN)_2]$	60.81	3.04	29.08	10.80	3.01	17.18	59.51
$[C_4C_1im]Br$	49.87	3.11	26.80	15.50	3.33	28.23	52.89
$[C_4C_1im][DMP]$	45.32	5.78	23.50	21.59	2.09	37.10	53.38
$[C_4C_1im]Cl$	43.10	4.46	21.94	19.92	3.11	33.67	49.53
IL + Na_2SO_4 + H_2O ABS							
$[C_4C_1im][CF_3SO_3]$	52.55	1.30	35.13	3.93	11.19	7.54	41.82
$[C_4C_1im][SCN]$	46.37	1.56	34.06	5.00	5.91	12.85	42.01
$[C_4C_1im][TOS]$	44.35	3.33	32.76	8.00	4.35	19.50	43.14
$[C_4C_1im][N(CN)_2]$	41.68	2.42	31.69	6.40	1.95	18.40	42.82
$[C_4C_1im]Br$	40.32	4.14	29.73	11.50	6.79	28.01	41.15
IL + $K_3C_6H_5O_7$ + H_2O ABS							
$[C_4C_1im][CF_3SO_3]$	50.78	2.91	35.00	10.00	3.02	24.36	52.36
$[C_4C_1im][SCN]$	56.77	2.57	30.00	9.60	9.61	16.64	49.21
$[C_4C_1im][TOS]$	51.24	6.21	32.06	15.39	6.34	27.71	49.79
$[C_4C_1im][N(CN)_2]$	52.21	3.62	24.70	15.13	6.98	22.55	49.03
$[C_4C_1im]Br$	53.25	5.78	30.00	22.00	9.65	36.2	53.16
$[C_4C_1im]Cl$	45.94	11.64	27.50	30.00	10.45	46.97	50.08

[a] $[IL]_M$, $[IL]_{IL}$ and $[IL]_{salt}$ correspond to IL weight fraction percentages in the initial mixture, and IL- and salt-rich phases, respectively; $[salt]_M$, $[salt]_{IL}$ and $[salt]_{salt}$ correspond to salt weight fraction percentages in the initial mixture, and IL- and salt-rich phases, respectively.

and 25 °C for 30 min. To guarantee the complete separation of the ABS coexisting phases and DNP-amino-acid partition, the systems were centrifuged at 25 °C in a VWR Micro Star 17 microcentrifuge, for 30 min at 3500 rpm. Finally, samples of the IL- and salt-rich phases were collected and diluted for further analysis by UV-spectroscopy at 362 nm, using a BioTeck Synergy HT microplate reader. The DNP-amino-acid partition coefficients ($K_{DNP\text{-}AA}$) were determined through the slope of the straight line obtained when the absorbances in the top phase are plotted against the absorbances in the bottom phase, while considering the dilution factors used.

Kamlet–Taft parameters determination

The probes *N*,*N*-diethyl-4-nitroaniline (1), 4-nitroaniline (2) and pyridine-*N*-oxide (3) were used to determine the dipolarity/polarizability, π*, hydrogen-bond (acceptor) basicity, β, and hydrogen-bond (donor) acidity, α, of the coexisting phases of the studied ABSs. For each mixture, a total of three replicates were prepared in Eppendorf tubes. After the centrifugation and the collection of a sample of each phase, *N*,*N*-diethyl-4-nitroaniline (≈0.30 mg), 4-nitroaniline (≈0.30 mg) and pyridine-*N*-oxide (0.25 mol dm^{-3}) were added. After agitation in a vortex mixer, the samples containing the probes *N*,*N*-diethyl-4-nitroaniline and 4-nitroaniline were scanned in a UV-Vis spectrophotometer (BioTeck Synergy HT microplate reader) at 25 °C to determine the longest wavelength absorption band of each probe in both phases. The β and π* solvatochromic parameters were determined by the following equations:

$$\beta = \frac{\left(\Delta\nu^{IL} - \Delta\nu^{cyclohexane}\right) \times 0.76}{\Delta\nu^{DMSO} - \Delta\nu^{cyclohexane}} \quad (13)$$

$$\Delta\nu^{i} = \nu_1^{i} - \nu_2^{i} \quad (14)$$

$$\pi^* = \frac{\nu_1^{IL} - \nu_1^{cyclohexane}}{\nu_1^{DMSO} - \nu_1^{cyclohexane}} \quad (15)$$

where ν_n^i is the experimental wavenumber in 10^3 cm^{-1} of probe *n* in the solvent *i*. Analyses were carried out in triplicate and the average standard deviation for each wavelength measured was always below 0.5 nm, for both probes.

The samples containing the probe pyridine-*N*-oxide were analyzed using ^{13}C nuclear magnetic resonance (NMR) in neat solvent with a Bruker Avance 300 at 300.13 MHz. Deuterium oxide (D_2O) was the solvent and trimethylsilyl propanoic acid (TSP) was the internal reference. The ^{13}C NMR chemical shifts $\delta(C_i)$ in ppm of the carbon atoms in positions *i* = 2 and 4 of pyridine-*N*-oxide (formula II) were determined, and α was calculated using eqn (16):[36,37]

$$\alpha = 0.15 \times d_{24} + 2.32 \quad (16)$$

with $d_{24} = \delta_4 - \delta_2$, $d_{34} = \delta_4 - \delta_3$ and δ_i the chemical shift of pyridine-*N*-oxide carbon *i*. The analyses were carried out in duplicate and the average standard deviation for each chemical shift was always below 0.02 ppm.

Solvatochromic solvent parameters of pure water and pure ILs were also determined using the same probes and procedures for comparison purposes.

COSMO-RS

The IL hydrogen-bonding interaction energies, E_{HB}, electrostatic-misfit interactions, E_{MF}, and van der Waals forces, E_{vdW}, were determined using the COSMO-RS thermodynamic model that combines quantum chemistry, based on the dielectric continuum model known as COSMO (COnductor-like Screening MOdel for Real Solvents), with statistical thermodynamic calculations. The standard process of COSMO-RS calculations employed in this work was previously described by Kurnia *et al.*[38] The quantum chemical COSMO calculations were performed with the TURBOMOLE 6.1 program package at the density functional theory (DFT) level, applying the BP functional B88-P86 with a triple-ζ valence polarized basis set (TZVP) and the resolution of identity standard (RI) approximation.[39] The COSMOthermX program using the parameter file BP_TZVP_C20_0111 (COSMOlogic GmbH & Co KG, Leverkusen, Germany) was used in all calculations.[40]

Results and discussion

Phase diagrams

The binodal curves of the ABSs formed by imidazolium-based ILs and the salts K_2CO_3, Na_2SO_4, and $K_3C_6H_5O_7$ were determined

at room temperature (≈25 °C). The detailed experimental procedure, data and graphical representations of the phase diagrams are given in the ESI.† Several experimental tie-lines (TLs), which give the composition of each phase for a given biphasic mixture, and their respective length (TLL), were additionally determined for each ABS. In Table 1 are given the TLs that will be used in further discussions. The remaining TLs are reported in the ESI.†

Gibbs free energy of a methylene group transfer between the ABS phases

Using a series of homologues of DNP-amino-acids (DNP-glycine, DNP-alanine, DNP-valine, and DNP-leucine), the Gibbs free energy of transfer of a methylene group, $\Delta G(CH_2)$, from the aqueous salt-rich to the aqueous IL-rich phase was determined for the ABSs listed in Table 1. The detailed data corresponding to the DNP-amino-acid partition coefficients are reported in the ESI.† The difference of the electrostatic properties and relative hydrophobicity of the coexisting phases (parameters C and E, respectively) were estimated by eqn (1), while $\Delta G(CH_2)$ was obtained from eqn (2). The respective results are reported in Table 2.

Independently of the salt used and pH, $\Delta G(CH_2)$ is always negative, meaning that the transfer of a non-polar $-CH_2$ group from the salt- to the IL-rich phase is favorable, and that methylene groups have a higher affinity to IL-rich than to salt-rich phases. The $\Delta G(CH_2)$ values of IL + K_2CO_3 and IL + $K_3C_6H_5O_7$ ABS range from −0.59 to −1.2 kJ mol^{-1} and −0.37 to −1.11 kJ mol^{-1}, respectively, while a more restricted range is observed for ABSs composed of Na_2SO_4 salt, namely from −0.54 to −0.7 kJ mol^{-1}.

The Gibbs free energies of transfer of a methylene group between the coexisting phases in IL-based ABSs were previously reported by Wu *et al.*[27,28] The authors evaluated the effect of the IL anion[27] and cation,[28] observing a strong dependency of $\Delta G(CH_2)$ on the IL hydrophobicity, and thus on the ability of the IL to form an ABS. Although the $\Delta G(CH_2)$ values reported in Table 2 are close to those reported by Wu *et al.*,[27,28] the reported behavior was not observed in the systems studied in this work. It should be noted that Wu *et al.*[27,28] determined the $\Delta G(CH_2)$ values at a fixed mixture composition, while in this work, a constant TLL was used (*cf.* ESI†). As the length of the TL increases, the two phases become more distinct in composition and properties, resulting in a change in the driving forces acting upon the molecules partitioning. Thus, when a fixed mixture composition is used in a set of systems that differ in the IL nature, not only the IL nature will influence the molecule extraction or the properties determination, but also the TLL. In the case of $\Delta G(CH_2)$, as the TLL increases (larger differences between the two phase compositions), the Gibbs free energy value also increases,[4,14] and similar results to those reported by Wu *et al.*[27,28] could be obtained. Yet, these would lead to a wrong interpretation of the relative hydrophobicities of the phases as the results are dominated by the TLL effect rather than by the nature of the phases.

Through the analysis of the $\Delta G(CH_2)$ results obtained for the imidazolium-based ILs studied here, it is not possible to identify any type of relation between this parameter and the IL concentration or its nature. Since the Gibbs free energy of transfer of a methyl group is only related to the relative hydrophobicity of the phases (*cf.* eqn (3)), it seems clear that at a fixed TLL, the hydrophobicity of IL-based ABS phases results from a delicate balance between the nature and concentration of all phase forming components – IL, salt and water – not being dominated by just one of them.

Table 2 Parameters C and E (eqn (1)), Gibbs free energy of transfer of a methylene group, $\Delta G(CH_2)$ (eqn (2)), and Kamlet–Taft parameters[a] and their differences between the coexisting phases of IL-based ABSs at 25 °C

IL	TLL	C	E	$\Delta G(CH_2)$ (kJ mol^{-1})	π_{IL}*	π_{salt}*	$\Delta\pi$*	α_{IL}	α_{salt}	$\Delta\alpha$	β_{IL}	β_{salt}	$\Delta\beta$
IL + K_2CO_3 + H_2O ABS													
[C_4C_1im][CF_3SO_3]	50.13	1.9 ± 0.1	0.29 ± 0.04	−0.7 ± 0.1	1.09	1.24	−0.15	1.13	1.34	−0.21	0.44	0.34	0.10
[C_4C_1im][SCN]	52.91	3.3 ± 0.1	0.31 ± 0.04	−0.8 ± 0.1	1.21	1.29	−0.08	1.17	1.34	−0.17	0.41	0.34	0.07
[C_4C_1im][TOS]	52.32	3.92 ± 0.02	0.237 ± 0.009	−0.59 ± 0.02	1.12	1.24	−0.12	1.21	1.33	−0.12	0.56	0.44	0.12
[C_4C_1im][$N(CN)_2$]	59.51	3.9 ± 0.2	0.50 ± 0.07	−1.2 ± 0.2	1.18	1.28	−0.10	1.15	1.33	−0.18	0.41	0.35	0.06
[C_4C_1im]Br	52.89	4.1 ± 0.2	0.45 ± 0.08	−1.12 ± 0.08	1.27	1.29	−0.02	1.21	1.31	−0.10	0.49	0.44	0.05
[C_4C_1im][DMP]	53.38	6.07 ± 0.03	0.46 ± 0.03	−1.13 ± 0.07	1.20	n.s.[b]	—	1.18	1.30	−0.12	0.59	n.s.[b]	—
[C_4C_1im]Cl	49.53	5.4 ± 0.1	0.33 ± 0.04	−0.8 ± 0.1	1.26	n.s.[b]	—	1.21	1.31	−0.10	0.53	n.s.[b]	—
IL + Na_2SO_4 + H_2O ABS													
[C_4C_1im][CF_3SO_3]	41.82	1.57 ± 0.04	0.24 ± 0.01	−0.60 ± 0.04	1.12	1.21	−0.09	1.17	1.35	−0.18	0.41	0.37	0.04
[C_4C_1im][SCN]	42.01	2.29 ± 0.02	0.218 ± 0.007	−0.54 ± 0.02	1.23	1.28	−0.05	1.23	1.35	−0.12	0.40	0.36	0.04
[C_4C_1im][TOS]	43.14	2.9 ± 0.1	0.30 ± 0.06	−0.7 ± 0.1	1.17	1.24	−0.07	1.26	1.35	−0.09	0.53	0.46	0.07
[C_4C_1im][$N(CN)_2$]	42.82	2.54 ± 0.01	0.218 ± 0.005	−0.54 ± 0.01	1.20	1.27	−0.07	1.21	1.34	−0.13	0.39	0.34	0.05
[C_4C_1im]Br	41.15	4.0 ± 0.1	0.25 ± 0.04	−0.6 ± 0.1	1.31	1.32	−0.01	1.26	1.36	−0.10	0.46	0.41	0.05
IL + $K_3C_6H_5O_7$ + H_2O ABS													
[C_4C_1im][CF_3SO_3]	52.36	2.21 ± 0.08	0.45 ± 0.03	−1.11 ± 0.07	1.13	1.23	−0.10	1.12	1.33	−0.21	0.50	0.46	0.04
[C_4C_1im][SCN]	49.21	1.90 ± 0.06	0.26 ± 0.02	−0.66 ± 0.06	1.26	1.30	−0.04	1.20	1.31	−0.11	0.41	0.39	0.02
[C_4C_1im][TOS]	49.79	2.36 ± 0.06	0.15 ± 0.02	−0.37 ± 0.06	1.15	1.18	−0.03	1.19	1.30	−0.11	0.54	0.50	0.04
[C_4C_1im][$N(CN)_2$]	49.03	2.56 ± 0.06	0.20 ± 0.02	−0.49 ± 0.06	1.19	1.25	−0.02	1.03	1.29	−0.26	0.38	0.38	0
[C_4C_1im]Br	53.16	2.71 ± 0.03	0.18 ± 0.01	−0.44 ± 0.03	1.31	1.33	−0.02	1.19	1.27	−0.08	0.53	0.50	0.03
[C_4C_1im]Cl	50.08	2.56 ± 0.01	0.202 ± 0.005	−0.50 ± 0.01	1.28	1.29	−0.01	1.13	1.22	−0.09	0.61	0.60	0.01

[a] The indexes M, IL and salt correspond to the initial mixture, and IL- and salt-rich phases, respectively. [b] Not soluble (n.s.).

The effect of a methylene group on ln(K) is independent of the nature of the partitioned solutes, meaning that E is a characteristic of the system under study. On the other hand, the contribution of the polar group of the solutes, represented by the constant C, depends on both the composition of the ABS and the solute being partitioned. Since a homologous series of solutes was used, the effect of solute nature will be constant and the differences observed in the parameter C result only from the composition of the studied systems. For the studied IL-based ABSs, the parameter C is considerably high, ranging between 1.9 and 6.07 for K_2CO_3-based ABSs, between 1.57 and 4.0 for Na_2SO_4-based ABSs, and between 1.90 and 2.71 for $K_3C_6H_5O_7$-based ABSs (*cf.* Table 2). These results suggest that the polar group of the DNP-amino-acids has a significant effect on their partition in IL-based ABSs.

In a previous work,[41] it was shown that the COSMO-RS[42–45] hydrogen bond energies, E_{HB}, correlate well with the hydrogen bond basicity of ILs. In this work, a linear relationship between the parameter C and E_{HB} of the ILs that comprise the K_2CO_3-, Na_2SO_4- and $K_3C_6H_5O_7$-based ABSs has additionally been found, as depicted in Fig. 1. Thus, this correlation indicates that for IL-based systems, C is mainly dependent on the chemical nature of the IL and is a result of polar/hydrogen bonding interaction differences of the coexisting phases. This also suggests that specific solute–IL interactions are present and have a significant effect on the partition of biomolecules in IL-based ABSs. However, while for K_2CO_3- and Na_2SO_4-based ABSs, the parameter C has a significant dependence on the IL E_{HB}, in $K_3C_6H_5O_7$-based ABSs, this effect is considerably weakened due to the strong salting-out nature of this salt. This suggests that the nature of the IL may be masked by the effect of the salt and that IL specific interactions play a more significant role in the solute partitioning in ABSs based on weaker salting-out salts, as demonstrated before with partition coefficient experimental data.[46]

The methylene group also plays a relevant role since the partition coefficients of DNP-amino-acids considerably increase with $n(CH_2)$ – *cf.* the ESI.† Nevertheless, considering the partition of DNP-leucine in the ABS composed of $[C_4C_1im][CF_3SO_3]$ + K_2CO_3 + H_2O, the contribution of the DNP-amino-acid polar group is represented by the value of C, *i.e.* 1.9, while the contribution of the methylene groups is equal to 1.7 (product of the parameter E, 0.29, and the number of equivalent methylene groups, in this case, 3.75).[3] Therefore, the contributions of both the polar and non-polar moieties are positive and similar. On the other hand, considering the partition of the same DNP-amino-acid in the $[C_4C_1im]Cl$ + K_2CO_3 + H_2O system, the contributions of both the polar and non-polar groups are 5.4 and 1.2, respectively, meaning that the influence of the polar groups is more than 4 times higher than that from the non-polar groups, suggesting that polar/hydrogen bonding interactions are the main driving force for this partition. Furthermore, this effect is more evident the smaller the number of CH_2 equivalent groups present in the DNP-amino-acids.

In Fig. 2, the ratio between the contribution of the polar group (*i.e.* polar/hydrogen bonding interactions) over the contribution of non-polar group (*i.e.* hydrophobic interactions) – $R_{polar/non\text{-}polar}$ – is represented for all DNP-amino-acid partitions in K_2CO_3-based ABSs. The results obtained for the Na_2SO_4- and $K_3C_6H_5O_7$-based ABSs are reported in the ESI.† The numbers of equivalent methylene groups for DNP-glycine, DNP-valine, DNP-alanine and DNP-leucine are 0.06, 1.31, 2.65 and 3.75,[3] respectively. Since DNP-glycine has a $n(CH_2)$ close to 0, the contribution of the hydrophobic interactions in its partition is almost null, and therefore the $R_{polar/non\text{-}polar}$ is high. Nevertheless, even when DNP-amino-acids with higher $n(CH_2)$ are considered, the contribution of the polar group is always higher than that of methylene groups (the ratio is always higher than unity) – as shown in Fig. 2. Furthermore, similarly to what was previously observed for the parameter C (Fig. 1), this ratio tends to increase with the E_{HB} of the IL, independently of the salt used, and even for ABSs based on the strong salting-out salt $K_3C_6H_5O_7$ – *cf.* ESI.† ILs with higher COSMO-RS hydrogen-bonding energies have a higher ability to hydrogen bond with the solutes and, consequently, the effect of the polar group in

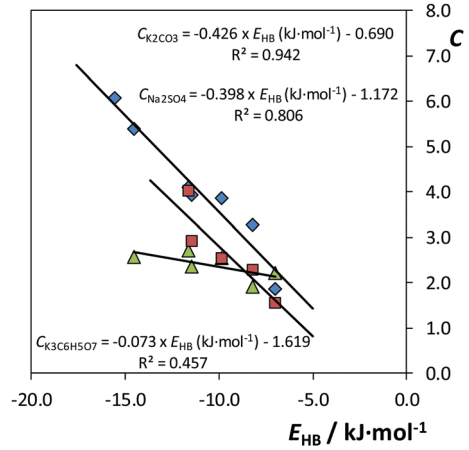

Fig. 1 Relationship between C and COSMO-RS hydrogen-bonding energies (E_{HB}) for K_2CO_3-based ABSs (■), Na_2SO_4-based ABSs (♦) and $K_3C_6H_5O_7$-based ABSs (▲).

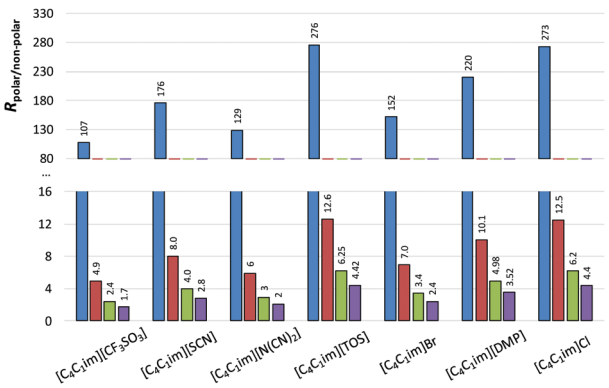

Fig. 2 Ratio of the contribution of polar (*i.e.* polar/hydrogen bonding interactions) and non-polar groups (*i.e.* hydrophobic interactions), $R_{polar/non\text{-}polar}$, of DNP-amino-acids (DNP-glycine – blue bars; DNP-valine – red bars; DNP-alanine – green bars and DNP-leucine – purple bars) in their partition in K_2CO_3-based ABSs.

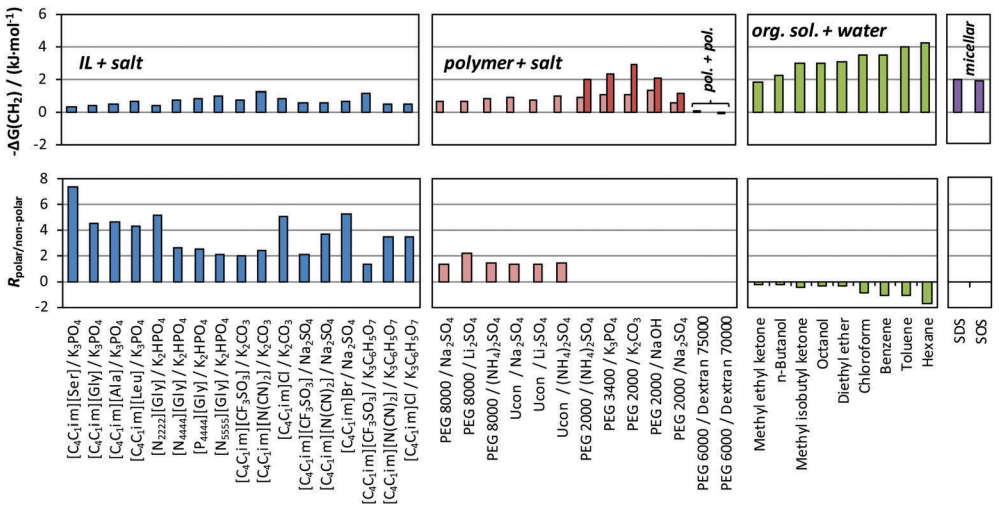

Fig. 3 Gibbs free energy ($\Delta G(CH_2)$) of transfer of a methylene group between the coexisting phases of different types of liquid–liquid systems and the ratio of solute polar and non-polar group contributions ($R_{polar/non\text{-}polar}$) in the partition of a molecule with $n(CH_2) \approx 4$: ABSs composed of IL/salt,[27,28] polymer/salt (light red – smallest TL; darker red – largest TL),[15,47] polymer/polymer,[3,13] and binary systems composed of organic solvents/water[17] and micellar-systems.[48] IL and compound abbreviations: 1-butyl-3-methylimidazolium L-serine ($[C_4C_1im][Ser]$), 1-butyl-3-methylimidazolium glycine ($[C_4C_1im][Gly]$), 1-butyl-3-methylimidazolium L-alanine ($[C_4C_1im][Ala]$) and 1-butyl-3-methylimidazolium L-leucine ($[C_4C_1im][Leu]$), tetramethylammonium glycine ($[N_{1111}][Gly]$), tetraethylammonium glycine ($[N_{2222}][Gly]$), tetrabutylammonium glycine ($[N_{4444}][Gly]$), tetrabutylphosphonium glycine ($[P_{4444}][Gly]$), tetrapentylammonium glycine ($[N_{5555}][Gly]$), polyethylene glycol (PEG), sodium dodecyl sulphate (SDS), and sodium octyl sulphate (SOS).

the partition of the DNP-amino-acids increases. However, if the system is constituted by an IL with lower E_{HB} values and a higher hydrophobic character, such as $[C_4C_1im][CF_3SO_3]$, the influence of the methylene groups in the partition becomes more important and the relative contributions of polar *vs.* non-polar interactions are more similar (ratio close to 1).

Fig. 3 depicts the comparison of $\Delta G(CH_2)$ values for different types of liquid–liquid systems previously reported in the literature. Since several factors could affect the $\Delta G(CH_2)$ values, whenever possible, $\Delta G(CH_2)$ values determined at similar TLLs were chosen. IL-based ABSs[27,28] present similar $\Delta G(CH_2)$ values to polymer–salt ABSs,[15,47] and considerably higher $\Delta G(CH_2)$ values than polymer–polymer systems.[3,13] Furthermore, binary systems composed of organic solvents and water[17] and micellar systems[48] are those that present the largest differences, due to the highly distinct chemical compositions of their phases. Whenever possible, ration of the contribution of the polar group over the non-polar group ($R_{polar/non\text{-}polar}$) was also calculated, which is represented in Fig. 3. The ratio between the polar and non-polar contributions is lower in the systems with higher $\Delta G(CH_2)$; this parameter shows that the polar group contribution is always slightly higher than that of the non-polar group in IL-based ABSs, while for polymer–salt ABSs, this ratio tends to be closer to 1. For organic solvent–water systems, the polar group displays a non-favorable impact on the solute partition for the organic phase ($C < 0$, and consequently $R_{polar/non\text{-}polar} < 0$). These results clearly reveal the different nature of IL-based ABSs when compared with other types of liquid–liquid systems.

Kamlet–Taft parameters

The Kamlet–Taft parameters – solvent dipolarity/polarizability, π^*, solvent hydrogen-bond (donor) acidity, α, and solvent hydrogen bond (acceptor) basicity, β – of IL-rich and salt-rich phases of IL–K_2CO_3, IL–Na_2SO_4 and IL–$K_3C_6H_5O_7$ ABSs, and their differences (Δ, calculated as the difference of a given parameter between the IL- and salt-rich phases), were determined at a constant TLL. Here, and hereafter, ''solvent'' refers to the global phase mixture, and not to an individual component, such as water, salt or IL. Each of the Kamlet–Taft parameters was obtained from a set of single probes. The obtained results are given in Table 2. Independently of the salt used, the salt-rich phases always present higher dipolarity/polarizability values than the IL-rich phases. Furthermore, the π^* value range is larger for the IL-rich than for the salt-rich phases, which present dipolarity/polarizability values close to those of pure water ($\pi_{H_2O}^* = 1.26$). Pure ILs usually display dipolarity/polarizability values considerably lower than water (*cf.* the ESI†), and therefore binary solutions of water and ILs are expected to present lower dipolarity/polarizability, as observed for the ABS IL-rich phases. However, these results are highly distinct from those observed for ABSs composed of polymers and/or salts, where in general both phases present a higher dipolarity/polarizability than water.[10,14] Although some conclusions could be drawn based on these results, from the solute partition point of view, the difference in the Kamlet–Taft parameters between the coexisting phases seems to be more relevant. The differences between the π^* values of the coexisting phases in IL-based ABSs are slightly higher than those observed in the polymer-based systems.[10,14] Furthermore, considering the $\Delta\pi^*$ values for K_2CO_3-, Na_2SO_4- and $K_3C_6H_5O_7$-based ABSs, there is a decrease in this difference with the increase in the IL hydrophilic character (ranked in terms of E_{HB}). These results suggest that non-specific dispersion interactions (van der Waals, among others) could be more significant in the partition of

solutes in IL-based than in polymer-based systems, and their impact could be tuned by the hydrophilic character of the IL.

The Kamlet–Taft parameter that seems to be less affected by the composition of the IL-based ABSs is the hydrogen bond donor acidity. For K_2CO_3- and Na_2SO_4-based ABSs, this parameter is almost constant in salt-rich phases with values close to that of pure water (α_{H_2O} = 1.36). However, for $K_3C_6H_5O_7$-based ABSs, a significant decrease in the salt-rich phase hydrogen bond acidity is observed in the systems composed of $[C_4C_1im]Cl$ and $[C_4C_1im]Br$, which could be a consequence of the high concentration of IL and salt present in both phases – *cf.* Table 1. In IL-rich phases, slight oscillations are observed for this parameter. Although the IL anion plays a dominant role, the hydrogen bond acidity is mainly determined by the IL cation, which justifies the small variations observed for this parameter in the studied systems. However, the differences between the coexisting phases ($\Delta\alpha$) are considerably higher than those observed for the dipolarity/polarizability and the hydrogen bond basicity. This behavior is similar to that observed in polymer–salt-based ABSs.[10,14]

Similarly to polymer–polymer- and polymer–salt-based ABSs,[9,10,14] the hydrogen bond basicity values of IL-based ABS coexisting phases are considerably higher than those of pure water (*cf.* the ESI†), with IL-rich phases presenting higher values than salt-rich phases. ILs present a considerably higher hydrogen-bond acceptor ability than water, meaning that their presence in an aqueous solution will increase the β value of the mixture. The hydrogen-bond acceptor ability is mainly controlled by the IL anion, justifying the large variations observed in β for the various systems studied. As observed for dipolarity/polarizability, also $\Delta\beta$ for K_2CO_3-based ABSs seems to decrease with the IL hydrophobicity. However, a clear tendency was not identified for Na_2SO_4- and $K_3C_6H_5O_7$-based ABSs.

To better understand the Kamlet–Taft parameter variations on the phase diagram of the IL-based ABSs, a more comprehensive analysis was carried out for the water–$[C_4C_1im][TOS]$–K_2CO_3 ternary system. The Kamlet–Taft parameters were determined in binary solutions of $[C_4C_1im][TOS]$ + water and K_2CO_3 + water, and in monophasic and biphasic ternary mixtures of $[C_4C_1im][TOS]$–K_2CO_3 ABSs. The compositions of each mixture are reported in the ESI.† The π^*, α and β parameters are represented as a contour plot on the ternary phase diagram of the $[C_4C_1im][TOS]$–K_2CO_3 ABS in Fig. 4.

According to Fig. 4A, the dipolarity/polarizability is mostly affected by water and K_2CO_3 concentrations. The addition of salt to highly diluted aqueous solutions slightly increases the value of π^*, but when the water concentration is below 80 wt%, the dipolarity/polarizability significantly decreases. On the other hand, the hydrogen-bond donor ability of the ternary mixture seems to be ruled by the water content (Fig. 4B). Although weaker, a similar tendency is observed for the hydrogen-bond acceptor ability (Fig. 4C). Concerning the TLL effect on the Kamlet–Taft parameters, the coexisting phases present symmetrical behaviors. For instance, the π^* of salt-rich phases increases and in IL-rich phases, it decreases with the TLL increase (Fig. 4A). A similar behavior was observed for the hydrogen-bond acceptor ability (Fig. 4C). In fact, as the IL concentration in the salt-rich phase decreases with the increase in the TLL, π^* and β values for this phase became closer to pure water. The increase in IL concentration in the IL-rich phase induces the opposite behavior. Thus, π^* and $\Delta\beta$ significantly increase with the TLL, contrary to what is observed for ABSs composed of polymers and salts, where these two parameters are essentially independent of the TLL.[10,14] It was previously shown that in polymer–polymer or polymer–salt ABSs, the solvatochromic probes do not specifically interact with the phase-forming components (salts and/or polymers).[49] However, the results here reported indicate that specific IL–solvatochromic probes interactions occur in IL-based ABSs, playing a significant role in the solvatochromic behavior of the probes.

Concerning the α and $\Delta\alpha$ of the coexisting phases, they present a similar behavior to that previously observed for polymer–salt ABSs.[10,14] The salt rich-phase displays a hydrogen bond acidity close to pure water and independent of the TLL, while the IL-rich phase value decreases considerably with the TLL. Since the water content of the salt-rich phases is almost constant, while it changes considerably in IL-rich phases with the increase of TLL, these trends are probably related to the water concentration in the phases.

As previously mentioned, the Kamlet–Taft parameter differences between the coexisting phases in ABSs are relevant factors to understand the partition of a solute. ABSs constituted by ILs and salts present a considerably broader variation of both non-specific and specific interactions, suggesting that this type of systems could be seen as a good option for the separation of molecules and compounds in which their partition could be ruled by specific interactions. Furthermore, in contrast to those observed in polymer-based systems,[10,14] these differences are strongly dependent on the type and concentrations of IL and salt as well as on the concentration of water that comprise the system, suggesting that IL-based ABSs can be tuned for the enhanced and selective extraction of a specific solute.

Relations between the various parameters studied

Previous studies on the characterization of polymer–polymer[12,50] and polymer–salt ABSs[51,52] have shown that (i) both *E* and *C* parameters could be correlated by a linear combination of solvent properties of the coexisting phases of the ABSs, and (ii) solute partition could be adequately described through a modified solvatochromic equation, based on eqn (3). These results led to the conclusion that solute partition in polymer–polymer and polymer–salt ABSs is mainly driven by solute–solvent interactions.[12,50–52]

Analysis of the results obtained in the present work using IL-based ABSs shows that no such correlations could be derived. For example, the description of the *E* parameter with the solvent properties $\Delta\pi^*$, $\Delta\alpha$, and $\Delta\beta$ for the 16 ABSs reported (Table 2) gives a correlation coefficient of 0.14, while for the *C* parameter, using the same procedure within the same ABSs gives a correlation coefficient of 0.58 – *cf.* the ESI.† These results suggest that the driving forces for solute partition in IL-based ABSs are different from conventional polymer-based ABSs.

The concept of solute–solvent interactions as the main driving force for solute partition in ABSs is widely recognized

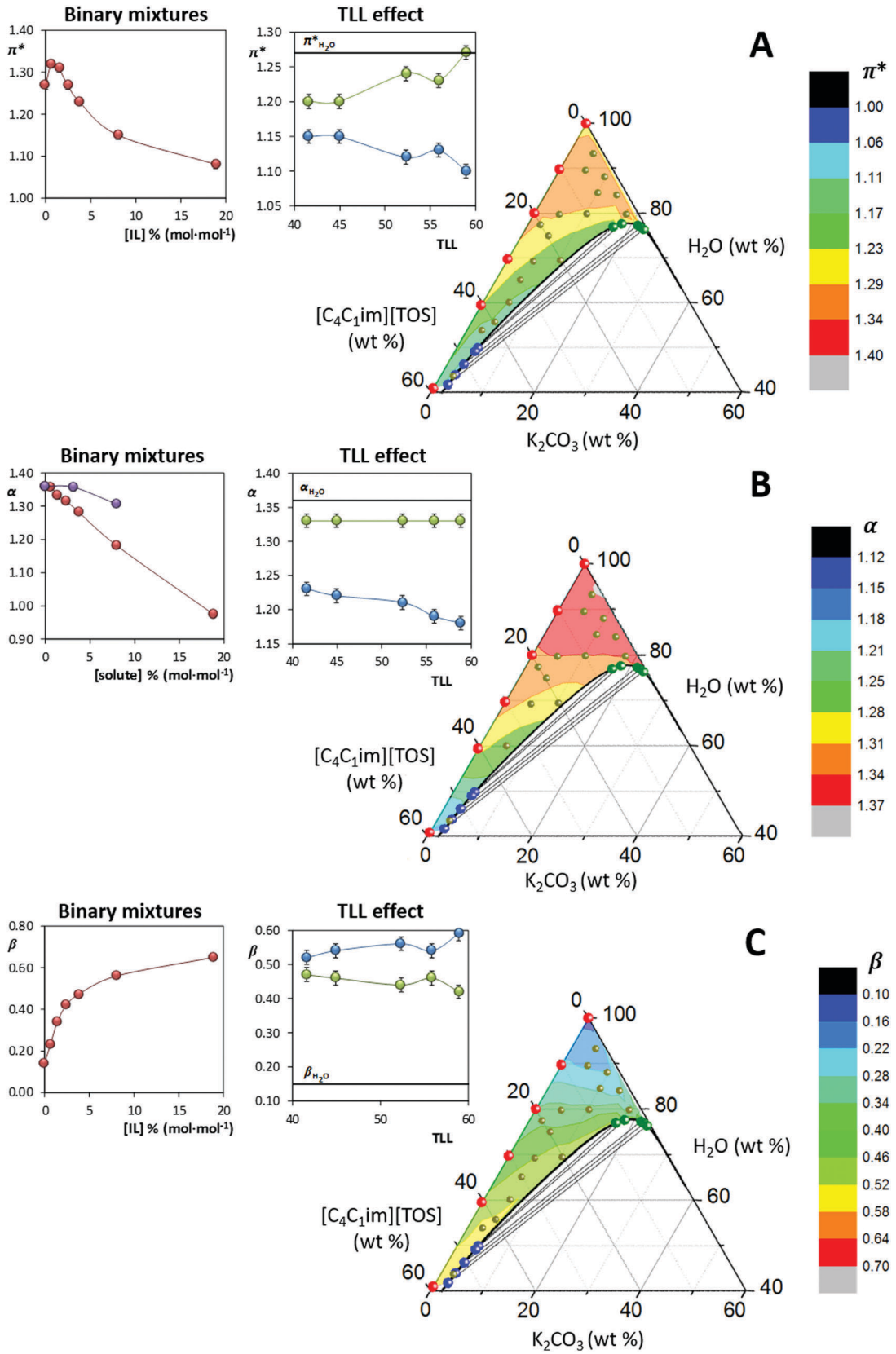

Fig. 4 The effect of ABS composition in the Kamlet–Taft parameters: (A) π*, (B) α, and (C) β. $[C_4C_1im][TOS]$–K_2CO_3-based ABSs: binary mixtures of $[C_4C_1im][TOS]$ and water (red circles), binary mixtures of K_2CO_3 and water (purple circles); IL-rich phases (blue circles); salt-rich phases (green circles).

not to be applicable to systems containing charged polymers or polymers with specific ligands.[53,54] In these systems, the partition is driven by solute–ligand specific interactions, similar to what is observed in IL-based ABSs,[55,56] and in polymer–salt ABSs for which ILs were used as additives.[57] In these works, it was shown that the presence of ILs as phase-forming components or simply as additives results in significant improvement in the ABS extraction performance. Specific solute–IL interactions in aqueous media have been recently reported by us,[58] demonstrating that ILs act as hydrotropes. By dynamic light scattering (DLS), molecular dynamics (MD) simulation and nuclear magnetic resonance (NMR), it was shown that the enhanced solubility of sparingly soluble solutes in water is driven by the formation of solute–IL aggregates, and that this IL-mediated hydrotropic effect is also solute-dependent.

Considering these previous observations[58] and the high partition coefficients or extraction efficiencies obtained with IL-based ABSs, we analyzed the partition data obtained in the present work (i) in the absence of an IL-mediated hydrotropic effect, and (ii) in the presence of a moderate IL-mediated hydrotropic effect, also by the application of a modified solvatochromic equation, based on eqn (3). In the absence of an IL-mediated hydrotropic effect, similarly to what is observed in polymer–polymer ABSs, solute partition in IL-based ABSs is mainly driven by solute–solvent interactions. On the other hand, when the partition occurs in the presence of a moderate IL-mediated hydrotropic effect, the solute partition is governed by a synergistic effect of both the solute–solvent and solute–IL specific interactions. The results obtained are illustrated by eqn (17) for the $[C_4C_1im][SCN]$- and $[C_4C_1im][N(CN)_2]$-based ABSs, and by eqn (18) for the $[C_4C_1im][SCN]$-, $[C_4C_1im][N(CN)_2]$-, $[C_4C_1im][TOS]$- and $[C_4C_1im][CF_3SO_3]$-based ABSs:

$$\ln(K_{\text{DNP-Gly}}) = 0.1_{\pm 0.1} - 25_{\pm 1}\Delta\pi^* - 7.7_{\pm 0.5}\Delta\alpha$$
$$n = 5,\ r^2 = 0.9971,\ F = 348.7,\ \text{SD} = 0.06,$$
$$p(0) = 0.5;\ p(\Delta\pi^*) = 0.002;$$
$$p(\Delta\alpha) = 0.005;\ \text{outl.: } [C_4C_1im][SCN]\text{–}Na_2SO_4\ \text{ABS}; \quad (17)$$

$$\ln(K_{\text{DNP-Gly}}) = 16_{\pm 3} - 20_{\pm 3}\Delta\pi^* - 8_{\pm 2}\Delta\alpha - 1.5_{\pm 0.2}E_{\text{HB}} - 2.1_{\pm 0.4}E_{\text{MF}} - 1.2_{\pm 0.2}V_{\text{dW}}$$
$$n = 11,\ r^2 = 0.9562,\ F = 21.8,\ \text{SD} = 0.22,\ p(0) = 0.003;$$
$$p(\Delta\pi^*) = 0.0005;\ p(\Delta\alpha) = 0.01;\ p(E_{\text{HB}}) = 0.0008;$$
$$p(E_{\text{MF}}) = 0.003;\ p(E_{\text{vdW}}) = 0.003;$$
$$\text{outl.: } [C_4C_1im][CF_3SO_3]\text{–}K_2CO_3\ \text{ABS}, \quad (18)$$

where n is the number of experimental $\ln(K)$ values; r is the correlation coefficient; F is the ratio of variance; SD is the standard deviation; p is the common statistic p-value based on the null hypothesis; "outl." is an outlier in the correlation; all the other parameters are as defined above.

The results illustrated by eqn (17) indicate that in the presence of the $[SCN]^-$ and $[N(CN)_2]^-$ anions, regardless of the salt used in the formation of the ABSs, no solute–IL specific interactions seem to be present, and consequently, partition data can be adequately described by the solvent parameters $\Delta\pi^*$ and $\Delta\alpha$. These results are similar to those previously described for polymer–polymer and polymer–salt ABSs,[12,50–52] and seem to indicate that DNP-amino-acid partition in $[C_4C_1im]SCN$- and $[C_4C_1im][N(CN)_2]$-based ABSs is governed by solute–solvent interactions. However, in the presence of $[TOS]^-$ and $[CF_3SO_3]^-$ anions, the experimental data can only be adequately described by introducing as additional parameters the COSMO descriptors E_{HB}, E_{MF} and E_{vdW}, as illustrated by eqn (18). These parameters are estimated through COSMO-RS, and they reflect the IL hydrogen-bonding interaction energies, E_{HB}, electrostatic–misfit interactions, E_{MF}, and van der Waals forces, E_{vdW}, accounting therefore for the ability of these ILs to establish specific interactions and thus for solute–IL specific interactions. Similar results were obtained for the remaining DNP-amino-acids, and for the E and C parameters – *cf.* the ESI.†

In summary, from the overall results obtained in the present work, it is shown that the solute partitions in IL-based ABSs are a result of multiple effects arising from the solute–IL and solute–solvent interactions, which further depend on the IL chemical nature. The solute–IL specific interactions, both derived from hydrotropic effects or from the enhanced polarity resulting from the $R_{\text{polar/non-polar}}$ previously discussed, may thus explain some experimental observations of enhanced partitions and selectivities provided by IL-based ABSs.

Conclusions

With the aim of better understanding the molecular-level mechanisms that rule the partition of molecules/solutes in ABSs composed of ILs and salts, the Gibbs free energy of a methylene group transfer and the Kamlet–Taft parameters of the phases in equilibrium were here studied. The relative hydrophobicity of the coexisting phases of a wide range of ABSs composed of $[C_4C_1im]$-based ILs and K_2CO_3, Na_2SO_4 or $K_3C_6H_5O_7$ was determined by the partition of a series of DNP-amino-acids. It was found that the partition of DNP-amino-acids in IL–salt ABSs is mainly ruled by hydrogen-bond interactions with ILs, and that the nature of the ILs is more significant when weaker salting-out salts are used. How the Kamlet–Taft parameters of the coexisting phases of the ABSs – dipolarity/polarizability (π^*), hydrogen-bonding acidity (α) and hydrogen-bonding basicity (β) – change with their composition was additionally evaluated. ABSs constituted by ILs and salts display a considerably high variation of the Kamlet–Taft parameters between the coexisting phases, with a significant dependency on the type and concentration of IL and salt. Non-specific dispersion interactions could be tuned by the hydrophilic character of the IL, while $\Delta\beta$ seems to be mainly related to the IL anion nature. In the systems studied, $\Delta\alpha$ appears to be mainly dependent on the water concentration. The results obtained suggest that in IL-based ABSs, both specific and non-specific interactions are more favorable to the partition of biomolecules than in polymer-based systems, with specific solute–IL interactions presenting a high impact.

The correlations found for the DNP-amino-acid partition coefficients with both the solvent properties and the ability of the ILs to establish specific interactions (here evaluated by the IL interaction energies estimated by COSMO-RS as descriptors) suggest that the driving forces governing the solute partition in IL-based ABSs result from multiple solute–solvent non-specific interactions and solute–IL specific interactions, both derived from hydrotropic effects or from their enhanced polarity. Contrary to the dominant solute–solvent non-specific interactions present in conventional polymer-based ABSs, the presence of solute–IL specific interactions explains the high partition coefficients, extraction efficiencies, and selectivity usually observed in IL-based ABSs.

Conflicts of interest

There are no conflicts to declare.

Acknowledgements

This work was developed in the scope of the project CICECO-Aveiro Institute of Materials (Ref. FCT UID/CTM/50011/2013), financed by national funds through the FCT/MEC and when applicable co-financed by FEDER under the PT2020 Partnership Agreement. The authors also acknowledge FCT for the doctoral grants SFRH/BD/85248/2012, SFRH/BD/109765/2015, SFRH/BD/126202/2016, and SFRH/BD/130958/2017 of H. Passos, M. V. Quental, E. V. Capela, and T. B. V. Dinis, respectively, and post-doctoral fellowship SFRH/BPD/111113/2015 of P. P. Madeira. M. G. Freire acknowledges the European Research Council under the European Union's Seventh Framework Programme (FP7/2007–2013)/ERC grant agreement no. 337753.

Notes and references

1 P. Å. Albertsson, *Partition of cell particles and macromolecules*, John Wiley & Sons Inc., New York, 2nd edn, 1971.
2 H. Walter, D. E. Brooks and D. Fisher, *Partitioning in aqueous two-phase systems: theory, methods, use, and applications to biotechnology*, Academic Press, Orlando, Florida, 1985.
3 B. Y. Zaslavsky, *Aqueous two-phase partitioning: physical chemistry and bioanalytical applications*, Marcel Dekker Inc., New York, 1994.
4 K. E. Gutowski, G. A. Broker, H. D. Willauer, J. G. Huddleston, R. P. Swatloski, J. D. Holbrey and R. D. Rogers, *J. Am. Chem. Soc.*, 2003, **125**, 6632–6633.
5 M. G. Freire, A. F. M. Cláudio, J. M. M. Araújo, J. A. P. Coutinho, I. M. Marrucho, J. N. C. Lopes and L. P. N. Rebelo, *Chem. Soc. Rev.*, 2012, **41**, 4966–4995.
6 A. Frerix, P. Geilenkirchen, M. Müller, M.-R. Kula and J. Hubbuch, *Biotechnol. Bioeng.*, 2007, **96**, 57–66.
7 P. A. J. Rosa, A. M. Azevedo, S. Sommerfeld, W. Bäcker and M. R. Aires-Barros, *Biotechnol. Adv.*, 2011, **29**, 559–567.
8 B. Y. Zaslavsky, V. N. Uversky and A. Chait, *Biochim. Biophys. Acta*, 2016, **1864**, 622–644.
9 P. P. Madeira, C. A. Reis, A. E. Rodrigues, L. M. Mikheeva, A. Chait and B. Y. Zaslavsky, *J. Chromatogr. A*, 2011, **1218**, 1379–1384.
10 J. G. Huddleston, H. D. Willauer and R. D. Rogers, *Phys. Chem. Chem. Phys.*, 2002, **4**, 4065–4070.
11 P. P. Madeira, A. Bessa, L. Álvares-Ribeiro, M. R. Aires-Barros, A. E. Rodrigues and B. Y. Zaslavsky, *J. Chromatogr. A*, 2013, **1274**, 82–86.
12 P. P. Madeira, A. Bessa, D. P. C. de Barros, M. A. Teixeira, L. Álvares-Ribeiro, M. R. Aires-Barros, A. E. Rodrigues, A. Chait and B. Y. Zaslavsky, *J. Chromatogr. A*, 2013, **1271**, 10–16.
13 M. L. Moody, H. D. Willauer, S. T. Griffin, J. G. Huddleston and R. D. Rogers, *Ind. Eng. Chem. Res.*, 2005, **44**, 3749–3760.
14 O. Rodríguez, S. C. Silvério, P. P. Madeira, J. A. Teixeira and E. A. Macedo, *Ind. Eng. Chem. Res.*, 2007, **46**, 8199–8204.
15 S. C. Silvério, P. P. Madeira, O. Rodríguez, J. A. Teixeira and E. A. Macedo, *J. Chem. Eng. Data*, 2008, **53**, 1622–1625.
16 J. F. B. Pereira, A. Magri, M. V. Quental, M. Gonzalez-Miquel, M. G. Freire and J. A. P. Coutinho, *ACS Sustainable Chem. Eng.*, 2016, **4**, 1512–1520.
17 B. Y. Zaslavsky, L. M. Miheeva and S. V. Rogozhin, *J. Chromatogr. A*, 1981, **216**, 103–113.
18 B. Y. Zaslavsky, L. M. Miheeva and S. V. Rogozhin, *J. Chromatogr. A*, 1981, **212**, 13–22.
19 N. J. Bridges, K. E. Gutowski and R. D. Rogers, *Green Chem.*, 2007, **9**, 177–183.
20 C. Reichardt and T. Welton, *Solvents and solvent effects in organic chemistry*, Wiley-VCH, Weinheim, 4th edn, 2010.
21 M. A. Ab Rani, A. Brant, L. Crowhurst, A. Dolan, M. Lui, N. H. Hassan, J. P. Hallett, P. A. Hunt, H. Niedermeyer, J. M. Perez-Arlandis, M. Schrems, T. Welton and R. Wilding, *Phys. Chem. Chem. Phys.*, 2011, **13**, 16831–16840.
22 M. J. Kamlet and R. W. Taft, *J. Am. Chem. Soc.*, 1976, **98**, 377–383.
23 R. W. Taft and M. J. Kamlet, *J. Am. Chem. Soc.*, 1976, **98**, 2886–2894.
24 M. J. Kamlet, J. L. Abboud and R. W. Taft, *J. Am. Chem. Soc.*, 1977, **99**, 6027–6038.
25 M. T. Clough, C. R. Crick, J. Gräsvik, P. A. Hunt, H. Niedermeyer, T. Welton and O. P. Whitaker, *Chem. Sci.*, 2015, **6**, 1101–1114.
26 Y. Pei, J. Wang, K. Wu, X. Xuan and X. Lu, *Sep. Purif. Technol.*, 2009, **64**, 288–295.
27 C. Wu, J. Wang, H. Wang, Y. Pei and Z. Li, *J. Chromatogr. A*, 2011, **1218**, 8587–8593.
28 C. Wu, J. Wang, Z. Li, J. Jing and H. Wang, *J. Chromatogr. A*, 2013, **1305**, 1–6.
29 L. Crowhurst, P. R. Mawdsley, J. M. Perez-Arlandis, P. A. Salter and T. Welton, *Phys. Chem. Chem. Phys.*, 2003, **5**, 2790–2794.
30 C. Chiappe, C. S. Pomelli and S. Rajamani, *J. Phys. Chem. B*, 2011, **115**, 9653–9661.
31 C. Chiappe and D. Pieraccini, *J. Phys. Org. Chem.*, 2005, **18**, 275–297.
32 M. Y. Lui, L. Crowhurst, J. P. Hallett, P. A. Hunt, H. Niedermeyer and T. Welton, *Chem. Sci.*, 2011, **2**, 1491–1496.

33 S. P. M. Ventura, C. M. S. S. Neves, M. G. Freire, I. M. Marrucho, J. Oliveira and J. A. P. Coutinho, *J. Phys. Chem. B*, 2009, **113**, 9304–9310.
34 H. Passos, A. R. Ferreira, A. F. M. Cláudio, J. A. P. Coutinho and M. G. Freire, *Biochem. Eng. J.*, 2012, **67**, 68–76.
35 J. C. Merchuk, B. A. Andrews and J. A. Asenjo, *J. Chromatogr. B: Biomed. Sci. Appl.*, 1998, **711**, 285–293.
36 P. P. Madeira, H. Passos, J. Gomes, J. A. P. Coutinho and M. G. Freire, *Phys. Chem. Chem. Phys.*, 2017, **19**, 11011–11016.
37 H. Schneider, Y. Badrieh, Y. Migron and Y. Marcus, *Z. Phys. Chem.*, 1992, **177**, 143–156.
38 K. A. Kurnia, F. Lima, A. F. M. Cláudio, J. A. P. Coutinho and M. G. Freire, *Phys. Chem. Chem. Phys.*, 2015, **17**, 18980–18990.
39 Univ. Karlsruhe Forschungszentrum Karlsruhe GmbH, TURBOMOLE V6.1 2009, 1989–2007, 25 GmbH, since 2007, available from http//www.turbomole.com.
40 F. Eckert and A. Klamt, *COSMOtherm Version C2.1 Release 01.08*, Cosmol. GmbH Co. KG, Leverkusen, Ger., 2006.
41 A. F. M. Cláudio, L. Swift, J. P. Hallett, T. Welton, J. A. P. Coutinho and M. G. Freire, *Phys. Chem. Chem. Phys.*, 2014, **16**, 6593–6601.
42 A. Klamt and G. Schüürmann, *J. Chem. Soc., Perkin Trans. 2*, 1993, 799–805.
43 A. Klamt, *COSMO-RS from quantum chemistry to fluid phase thermodynamics and drug design*, Elsevier, Amsterdam, Boston, 2005.
44 A. Klamt, *J. Phys. Chem.*, 1995, **99**, 2224–2235.
45 A. Klamt and F. Eckert, *Fluid Phase Equilib.*, 2000, **172**, 43–72.
46 F. Hofmeister, *Arch. Exp. Pathol. Pharmakol.*, 1888, **XXV**, 1–30.
47 H. D. Willauer, J. G. Huddleston and R. D. Rogers, *Ind. Eng. Chem. Res.*, 2002, **41**, 2591–2601.
48 M. F. Vitha and P. W. Carr, *Sep. Sci. Technol.*, 1998, **33**, 2075–2100.
49 L. A. Ferreira, P. P. Madeira, L. Breydo, C. Reichardt, V. N. Uversky and B. Y. Zaslavsky, *J. Biomol. Struct. Dyn.*, 2016, **34**, 92–103.
50 P. P. Madeira, A. Bessa, J. A. Loureiro, L. Álvares-Ribeiro, A. E. Rodrigues and B. Y. Zaslavsky, *J. Chromatogr. A*, 2015, **1408**, 108–117.
51 P. P. Madeira, A. Bessa, L. Álvares-Ribeiro, M. R. Aires-Barros, C. A. Reis, A. E. Rodrigues and B. Y. Zaslavsky, *J. Chromatogr. A*, 2012, **1229**, 38–47.
52 N. R. da Silva, L. A. Ferreira, L. M. Mikheeva, J. A. Teixeira and B. Y. Zaslavsky, *J. Chromatogr. A*, 2014, **1337**, 3–8.
53 Q. Ma, Y. Song, J. W. Kim, H. S. Choi and H. C. Shum, *ACS Macro Lett.*, 2016, **5**, 666–670.
54 S. D. Flanagan and S. H. Barondes, *J. Biol. Chem.*, 1975, **250**, 1484–1489.
55 F. Ruiz-Ruiz, J. Benavides, O. Aguilar and M. Rito-Palomares, *J. Chromatogr. A*, 2012, **1244**, 1–13.
56 P. A. J. Rosa, A. M. Azevedo, I. F. Ferreira, J. de Vries, R. Korporaal, H. J. Verhoef, T. J. Visser and M. R. Aires-Barros, *J. Chromatogr. A*, 2007, **1162**, 103–113.
57 J. F. B. Pereira, Á. S. Lima, M. G. Freire and J. A. P. Coutinho, *Green Chem.*, 2010, **12**, 1661–1669.
58 A. F. M. Cláudio, M. C. Neves, K. Shimizu, J. N. Canongia Lopes, M. G. Freire and J. A. P. Coutinho, *Green Chem.*, 2015, **17**, 3948–3963.

